

Article

Expression of m6A Regulator Genes can Facilitate the Diagnosis of Chronic Heart Failure

Fang Zhou^{1,†}, Yang Yu^{2,†}, Yukun Li³, Jessica Chen⁴, Songnan Wen⁵, Nian Liu³, Xin Li³, Rong Bai^{6,7,*}, Wanyao Yan^{1,*}

¹Department of Pharmacy, Wuhan Fourth Hospital, 430033 Wuhan, Hubei, China

²Department of Cardiology, The Central Hospital of Wuhan, Tongji Medical College, Huazhong University of Science and Technology, 430014 Wuhan, Hubei, China

³Department of Cardiology, Beijing Anzhen Hospital, Capital Medical University, 100029 Beijing, China

⁴Department of Molecular, Cell, and Developmental Biology, University of California Los Angeles, Los Angeles, CA 90095, USA

⁵Department of Cardiovascular Medicine, Mayo Clinic, Scottsdale, AZ 85259, USA

⁶Division of Cardiology, Banner University Medical Center, University of Arizona College of Medicine, Phoenix, AZ 85006, USA

⁷Texas Cardiac Arrhythmia Institute, St. David's Medical Center, Austin, TX 78705, USA

*Correspondence: bairong74@gmail.com (Rong Bai); yanwanyao2023@163.com (Wanyao Yan)

†These authors contributed equally.

Submitted: 11 July 2023 Revised: 28 August 2023 Accepted: 7 September 2023 Published: 11 October 2023

Abstract

Background: RNA N6-methyladenosine (m6A) is the most common type of modification in eukaryotic mRNA. The relationship between m6A modification and disease has been studied extensively, but there have been few studies on chronic heart failure (CHF). This study investigated a possible role for m6A in the diagnosis of CHF. **Methods:** Seven candidate m6A regulators (writers: *WTAP* and *ZC3H13*; readers: *YTHDF3*, *FMRI*, *IGFBP1*, and *ELAVL1*; eraser: *FTO*) were identified using a random forest (RF) model and the GSE5406 dataset from the Gene Expression Omnibus database. A nomogram model was developed to predict the risk of CHF, while consensus clustering methodology assigned CHF samples into two m6A patterns (cluster A and cluster B) according to the 7 candidate m6A regulators. Principal component analysis was used to calculate an m6A score for each sample and to quantify m6A patterns. **Results:** Decision curve analysis and the nomogram model were used to obtain predictions that may be of clinical use. Patients in cluster B had higher m6A scores than patients in cluster A. Cluster B patients also had higher expression levels (ELs) of *IL-4*, *IL-5*, *IL-10* and *IL-13* than patients in cluster A, whereas cluster A patients had a higher EL for *IL-33*. The m6A cluster B pattern likely represents the ischemic heart failure (HF) disease group. **Conclusion:** m6A regulators are important in the pathogenesis of CHF associated with ischemic and idiopathic dilated cardiomyopathy, and may prove useful for the diagnosis and treatment of CHF.

Keywords

m6A; idiopathic dilated heart failure; ischemic heart failure; chronic heart failure

Introduction

The capacity for myocardial contraction is gradually weakened in chronic heart failure (CHF). In patients with CHF, the ejection and filling functions of the heart are damaged by several factors. In addition, blood perfusion to the body tissues and organs is decreased, and the circulation becomes congested. Progressive deterioration of cardiac function occurs in parallel with myocardial apoptosis and myocardial necrosis, with CHF being the terminal manifestation of various cardiovascular diseases. The age-adjusted incidence of CHF has decreased in developed countries, presumably reflecting the improved management of cardiovascular disease. However, the overall incidence of CHF remains high due to the aging population in these countries. Currently, the incidence of CHF in Europe is 3/1000 person-years in all age groups, and 5/1000 person-years in adults. CHF therefore affects approximately 1–2% of adults [1].

Of the 170 or more types of RNA modification, N6-methyladenosine (m6A) modification stands out as the most common reversible and dynamic transcriptional modification of eukaryotic mRNA. m6A accounts for about 50% of all methylated ribonucleotides and has major importance in cardiovascular disease [2]. The regulation of epigenomic m6A modification involves a dynamic and reversible process controlled by specific modulators known as specialized methyltransferases (writers), specialized demethylases (erasers), and m6A binding proteins (readers). These components play crucial roles in achieving precise control and interpretation of m6A modifications within the epigenome [3]. Genetic testing has been shown to improve the diagnosis of CHF and also provides information that can be used to reduce morbidity and improve the patients' quality of life [4–6]. Moreover, targeting the regulators of m6A

methylation may be a potential therapeutic approach for the treatment of heart failure (HF) [7,8]. However, additional research is required to determine more fully characterize the association between regulation of m6A methylation and CHF.

The aim of this work was to predict the risk of CHF by analyzing the expression of m6A regulators in the GSE5406 dataset from Gene Expression Omnibus (GEO). A model with 7 candidate m6A regulators was developed, namely the *WTAP*, *ZC3H13*, *YTHDF3*, *FMRI*, *IGFBP1*, *ELAVL1*, and *FTO* genes. Two m6A cluster patterns were identified, one of which (cluster B) may be related to the development of ischemic HF.

Methods

Data Acquisition

The gene expression dataset GSE5406 was obtained from GEO and was last updated in August 2018. It contains 210 enrolled patients, of which 194 are CHF patients (86 idiopathic dilated HF samples and 108 ischemic HF samples). The healthy control group (HC) contained 16 samples. CHF samples were collected from heart tissues during heart transplant surgery, and HC samples from unused donor hearts with normal left ventricle function. Following analysis of the HC and CHF groups, 20 m6A regulators were identified, including 6 writers (*METTL3*, *WTAP*, *ZC3H13*, *RBM15*, *RBM15B*, and *CBL1*), 1 eraser (*FTO*), and 13 readers (*YTHDC1*, *YTHDC2*, *YTHDF1*, *YTHDF2*, *YTHDF3*, *HNRNPC*, *FMRI*, *LRPPRC*, *HNRNPA2B1*, *IGFBP1*, *IGFBP2*, *IGFBP3*, and *ELAVL1*).

Analysis of Expression Levels (ELs) for m6A Regulators

The ELs for m6A regulators were RMA-normalized (log base 2 scale) and were analyzed using the “Pheatmap”, “Limma”, and “RCircos” packages. Heat maps, histograms, and the landscape of chromosomal positions of the m6A regulators were plotted (Fig. 1). Correlations between the ELs of writers and erasers were analyzed using Spearman correlation analysis (Fig. 2).

Development and Application of the Random Forest (RF) and Support Vector Machine (SVM) Models to Predict CHF

RF and SVM models were developed and used as training models to predict CHF. “Reverse Cumulative Distribution of Residual” (Fig. 3A), “Boxplots of Residual” (Fig. 3B), and “Receiver Operating Characteristic (ROC) curve” (Fig. 3C) were plotted. “RandomForest” package in R was employed to develop the RF model. From this, candidate CHF-associated m6A regulators were selected from the 20 m6A regulators to predict HF. The param-

eters “ntrees” and “mtry” were set at 500 and 2, respectively. Seven m6A regulators whose expression was significantly different between the CHF and HC groups were selected and subjected to importance analysis (Fig. 3D). These were Wilms’ tumor 1-associated protein (*WTAP*), zinc finger CCCH-type containing 13 (*ZC3H13*), YTH N6-methyladenosine RNA binding protein 1 (*YTHDF3*), fragile X mental retardation 1 (*FMRI*), insulin-like growth factor-binding protein 1 (*IGFBP1*), ELAV-like protein 1 (*ELAVL1*), and fat mass and obesity-associated protein (*FTO*).

Development of a Nomogram Model

A nomogram model to predict the risk of CHF was developed using the 7 candidate m6A regulators and employing the “rms” package in R. A calibration curve was utilized to demonstrate the consistency and coherence of the predicted probability against the actual probability. Decision curve analysis (DCA) was performed and a clinical impact curve was plotted to determine whether the decisions made by the model were beneficial for the patient (Fig. 4).

Grouping the m6A Regulators

Consensus clustering methodology was performed using the “ConsensusClusterPlus” package (reps = 50, pItem = 0.8, pFeature = 1, cluster Alg = “pam”, distance = “euclidean”, seed = 123456) in R to identify distinctions among the seven m6A regulators (Fig. 5). K = 2, 3, 4, 5, and 6 were selected to assign samples into various groups and to select the most suitable groupings. Two groups, cluster A and cluster B, were eventually established. m6A scores were calculated using principal component analysis (PCA) algorithms [9] as follows: m6A score = PC1i + PC2i, where PC1 and PC2 represent principal component-1 and principal component-2, respectively, and “i” represents differentially expressed gene (DEG) expression.

Differences in Enrichment and Relationships Amongst Immune Cells in CHF Patients According to m6A Groups

Differences in immune cell types in the different m6A groups were assessed using single-sample gene set enrichment analysis (ssGSEA) (Fig. 6). Heat maps of the different immune cell types were produced, and genes with markedly high or low ELs were identified. Subsequently, the different subtypes in immune cell enrichment in the high and low expression groups were analyzed.

Identification of Differentially Expressed Genes in m6A Groups, and Functional Enrichment Analysis

“Limma” and “VennDiagram” packages in R were utilized to screen DEGs in m6A cluster A and cluster B (Fig. 7). The screening criteria was set to $p < 0.05$ and

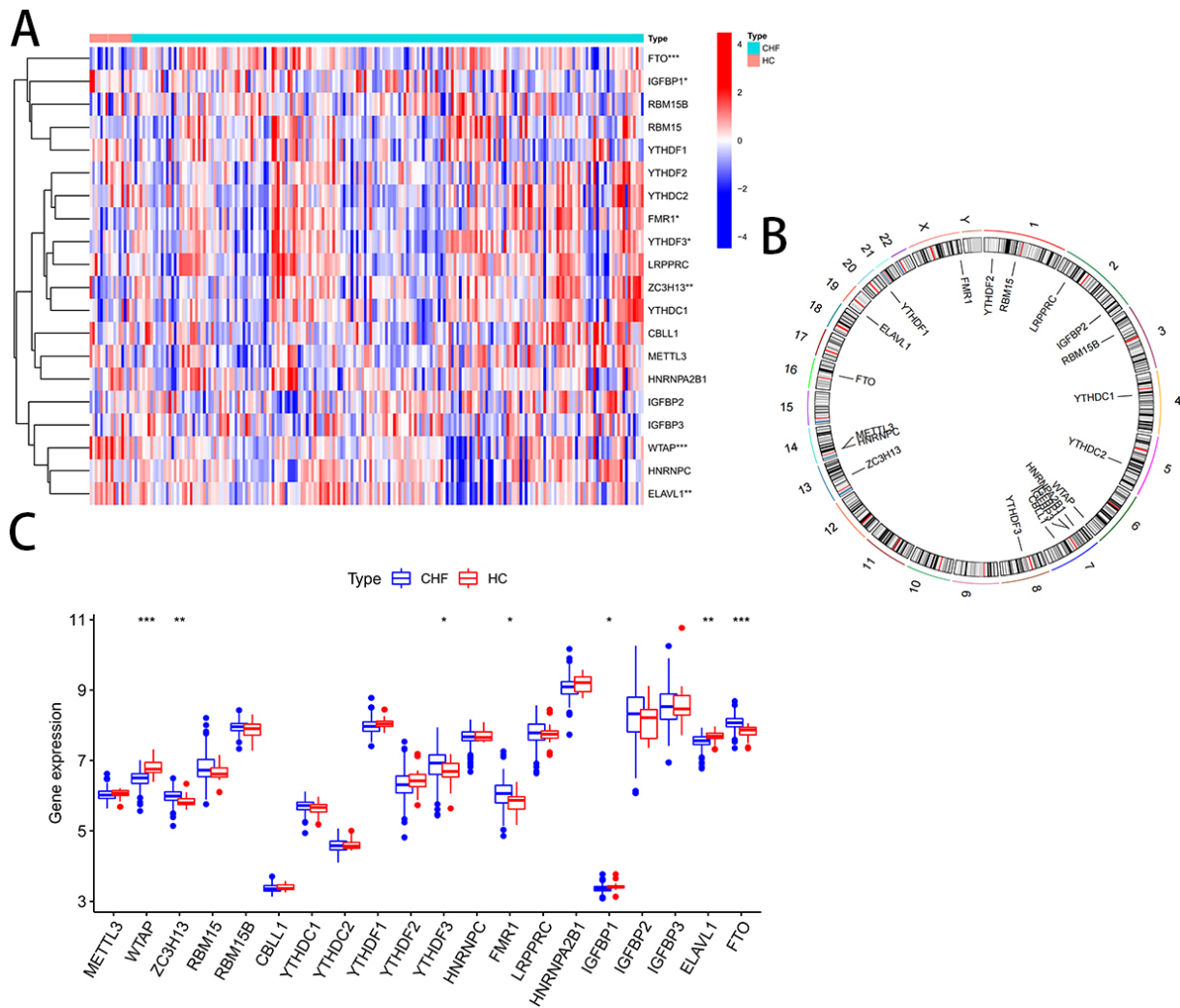


Fig. 1. Gene expression landscape of the 20 RNA N6-methyladenosine (m6A) regulators in chronic HF (CHF) and healthy control (HC) groups. (A) Expression heat map of the 20 m6A regulators in the CHF and HC groups. (B) Chromosomal positions of the 20 m6A regulators. (C) Differential expression histogram of the 20 m6A regulators in the CHF and HC groups. * $p < 0.05$, ** $p < 0.01$, and *** $p < 0.001$. CHF, chronic heart failure; HC, healthy control.

$\log_{2}FC > 1$ in order to classify samples into two groups: gene cluster (GC) A (GCA) and GCB. To identify possible mechanisms underlying the involvement of DEGs in CHF, “clusterProfiler” package in R was used to perform Gene Ontology (GO) functional enrichment analysis (FEA), and Kyoto Encyclopedia of Genes and Genomes (KEGG) enrichment analysis. An enrichment circle diagram was generated to illustrate these results, and Sankey diagrams were produced for m6A cluster A and cluster B, GCA and GCB, and m6A scores using the “ggalluvial” package in R (Fig. 8). ELs for *IL-2*, *IL-4*, *IL-5*, *IL-6*, *IL-10*, *IL-13*, and *IL-33* in the m6A cluster A and cluster B, and GCA and GCB, were visualized using the “GGpubr” and “reshape2” packages. In addition, *t*-tests were performed on the 7 candidate m6A regulators in the ischemic HF group and in the idiopathic dilated HF group to assess statistical differences between the m6A regulators in these groups.

Statistical Analysis

Wilcoxon tests were utilized to compare between groups. Statistical significance was set as $p < 0.05$, and all statistical analyses were performed using R4.1.2 and GraphPad 8.0 (GraphPad Software, Inc., San Diego, CA, USA).

Results

Expression Landscape of the 20 m6A Regulators in CHF

A total of 20 m6A regulators were identified in this study, including 6 writers, 1 eraser and 13 readers. The ELs of these m6A regulators in the CHF and HC groups are shown in Fig. 1A, and their chromosomal locations in Fig. 1B. The ELs of *ZC3H13*, *YTHDF3*, *FMR1*, and

Table 1. Biological functions exerted by 7 m6A regulators in cardiovascular diseases.

Name	Function	Biological function	Reference
<i>WTAP</i>	Writer	inhibits the proliferation and migration of vascular smooth muscle cells through m6A-mediated expression upregulation of p16	[12]
<i>ZC3H13</i>	Writer	promotes the malignant behavior of hepatoma carcinoma cells through PKM2-dependent glycolysis signaling	[10]
<i>FTO</i>	Eraser	attenuates ischemia-induced cardiac dysfunction in HF mice	[8]
<i>IGFBP1</i>	Reader	modulates the cellular processes implicated in short-term ventricular remodeling of the infarcted myocardium	[13]
<i>FMR1</i>	Reader	overexpression alleviates oxidative stress and apoptosis in injured H9c2 cardiomyocytes	[11]
<i>YTHDF3</i>	Reader	modulates cardiomyocytes and negatively regulates cardiac gene expression	[14]
<i>ELAVL1</i>	Reader	regulates cardiomyocyte proliferation and apoptosis	[15]

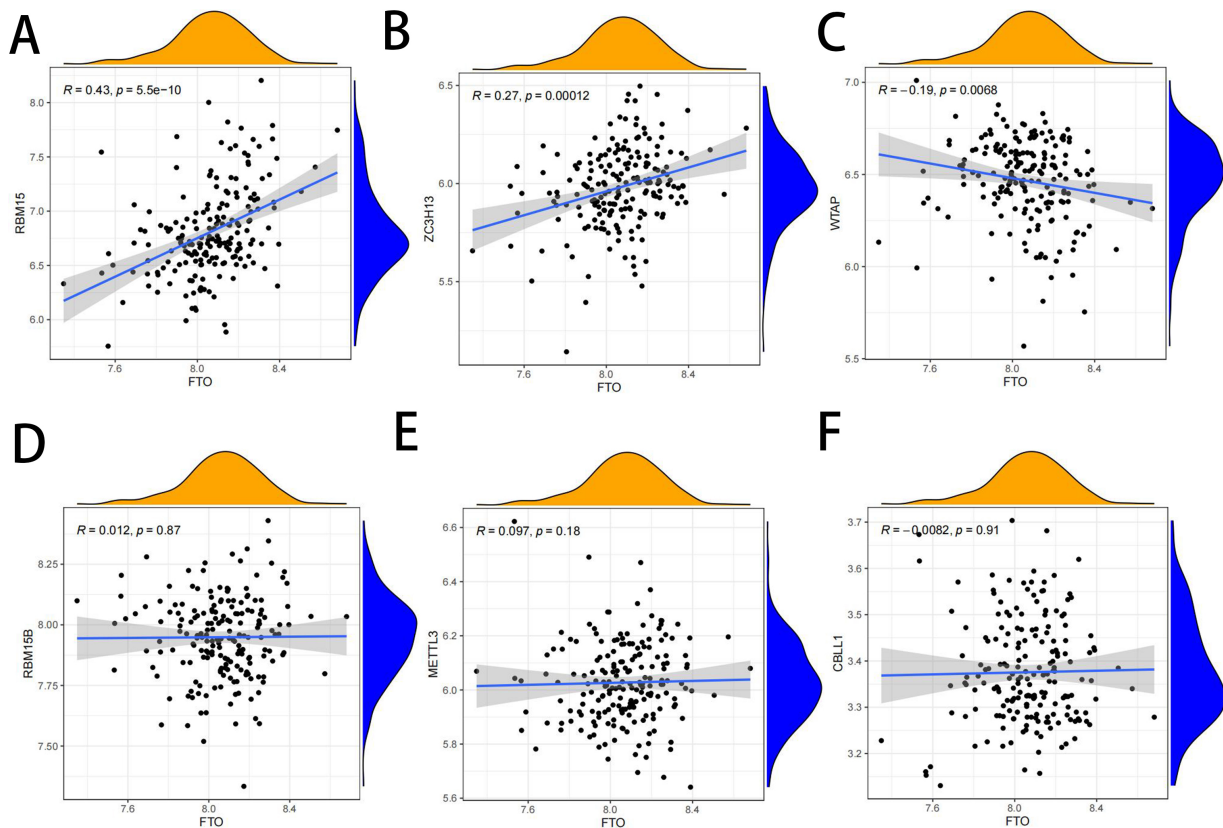


Fig. 2. Correlations between ELs of writer and eraser genes in chronic HF. (A–F) Writer genes: *METTL3*, *WTAP*, *ZC3H13*, *RBM15*, *RBM15B*, *CBL1*; eraser gene: *FTO*.

FTO were increased in the CHF group compared to the HC group, whereas the ELs of *ELAVL1*, *WTAP*, and *IGFBP1* were increased in the HC group relative to the CHF group (Fig. 1C). The biological functions exerted by the 7 m6A regulators in cardiovascular diseases are shown in Table 1, Ref. [8,10–15]).

m6A regulators. A moderately positive correlation was found between the ELs of *RBM15* and *FTO* in CHF patients ($R = 0.43$, $p < 0.0001$; Fig. 2A). The ELs of *ZC3H13* and *FTO* were also weakly positively correlated ($R = 0.27$, $p < 0.0001$; Fig. 2B). No other significant correlations were observed between writers and the *FTO* eraser (Fig. 2C–F).

Correlations between the Expression Levels of Writer and Eraser m6A Regulators in CHF

Spearman correlation analysis was used to examine correlations between the ELs of writer (*METTL3*, *WTAP*, *ZC3H13*, *RBM15*, *RBM15B*, and *CBL1*) and eraser (*FTO*)

Appropriateness of RF and SVM Models for Selecting m6A Regulators to Predict CHF

As shown in Fig. 3A,B, “Reverse cumulative distribution of residual” and “Boxplots of residual” suggested the RF model had smaller residuals than the SVM model. The

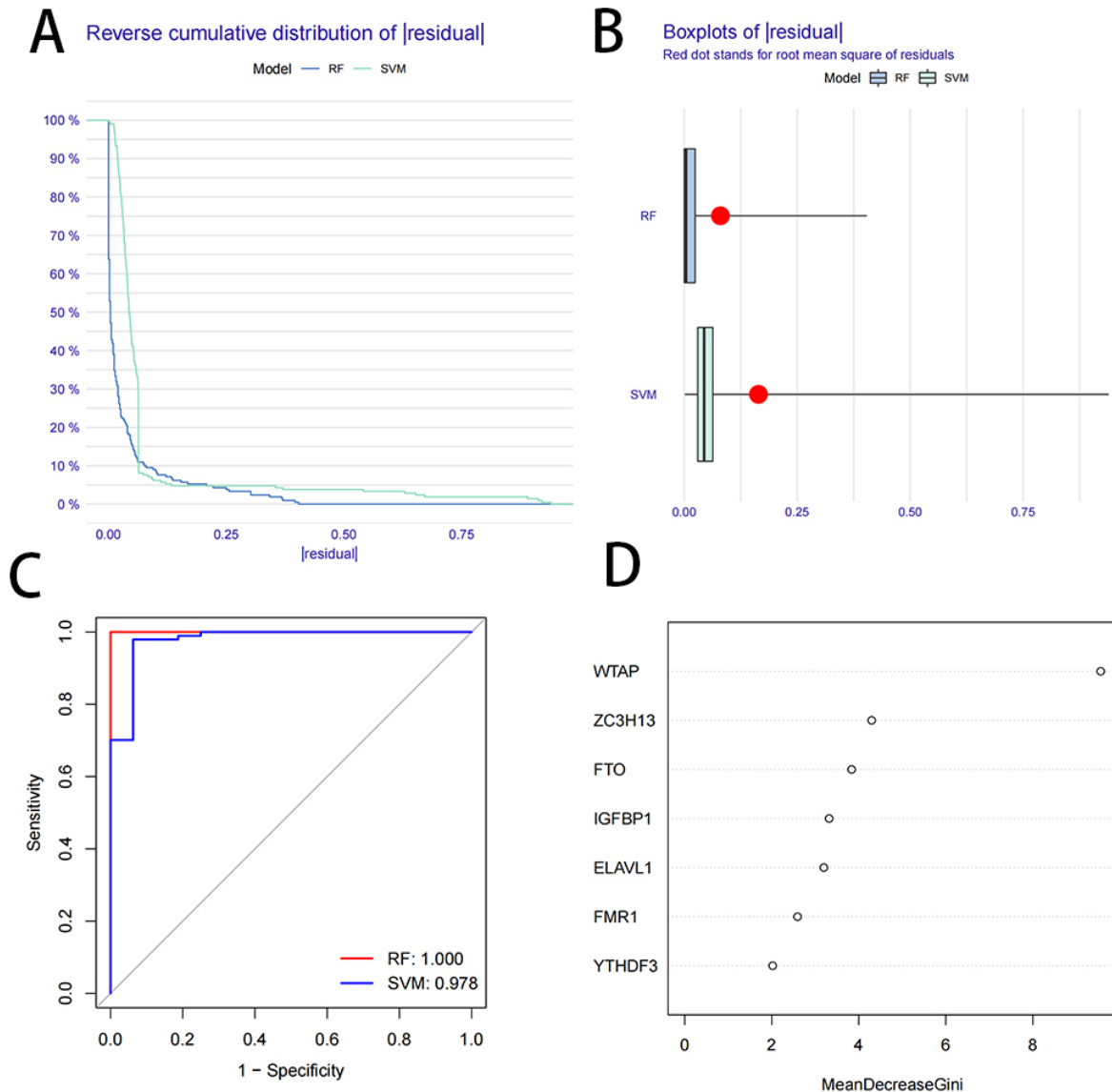


Fig. 3. Construction and screening of the random forest (RF) and support vector machine (SVM) models. (A) Reverse cumulative distribution of residual with the RF and SVM models. (B) Boxplots of residual with the RF and SVM models. (C) ROC curves for the RF and SVM models. (D) Relative importance of the 7 m6A regulators based on the RF model. RF, random forest; SVM, support vector machine; ROC, receiver operating characteristic.

RF model was therefore the better at predicting CHF and was utilized in the subsequent analyses. The RF model was further validated by the value of the “area under the curve” in ROC analysis. This showed the sensitivity and specificity of the RF model were both superior to those of SVM model (Fig. 3C). The importance of the 7 selected m6A regulators were ranked as follows (Fig. 3D): *WTAP* > *ZC3H13* > *FTO* > *IGFBP1* > *ELAVL1* > *FMR1* > *YTHDF3*.

Appropriateness of the Nomogram Model for Predicting CHF

The nomogram model developed using the 7 selected m6A regulators (Fig. 4A) was found to have good predictive value for predicting CHF risk (Fig. 4B). DCA indicated

that decision-making with the nomogram model could benefit CHF patients (Fig. 4C), since the curve remained above the risk threshold and the standardized net benefit. The nomogram model demonstrated favorable predictive ability, as evidenced by the clinical impact curve (Fig. 4D).

Two Distinct m6A Expression Patterns Emerge from the Seven Selected m6A Regulators

Consensus clustering methodology revealed that two distinct m6A patterns, cluster A and cluster B, emerged from the ELs of the 7 selected m6A regulators in the 194 CHF samples (Fig. 5A–E). Clusters A and B contained 138 and 56 samples, respectively. Heat maps and histograms show the differential ELs of the 7 selected m6A regulators

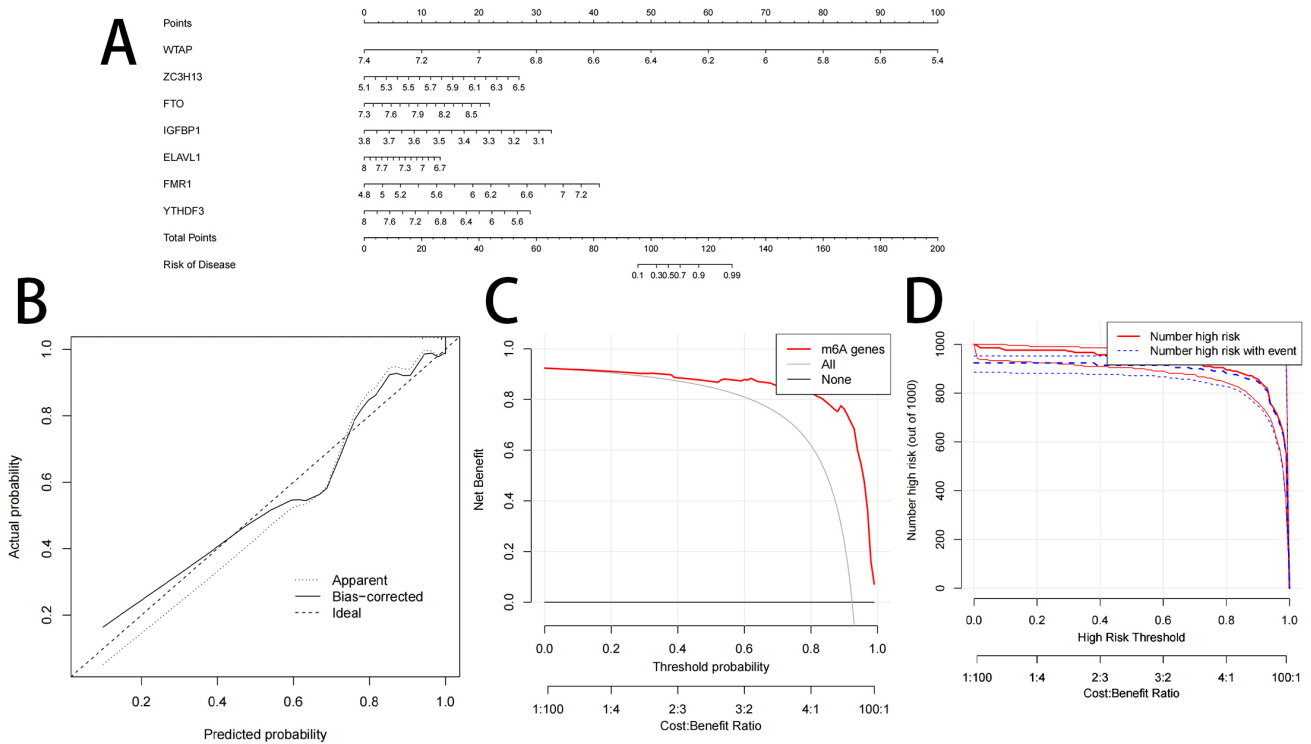


Fig. 4. Construction of the Nomogram Model. (A) Construction of the nomogram model based on the 7 selected candidate m6A regulators. (B) Predictive ability of the nomogram model as revealed by the calibration curve. (C) Decisions based on the nomogram model, showing the model could benefit CHF patients. (D) Favorable predictive ability of the nomogram model, as assessed by the clinical impact curve.

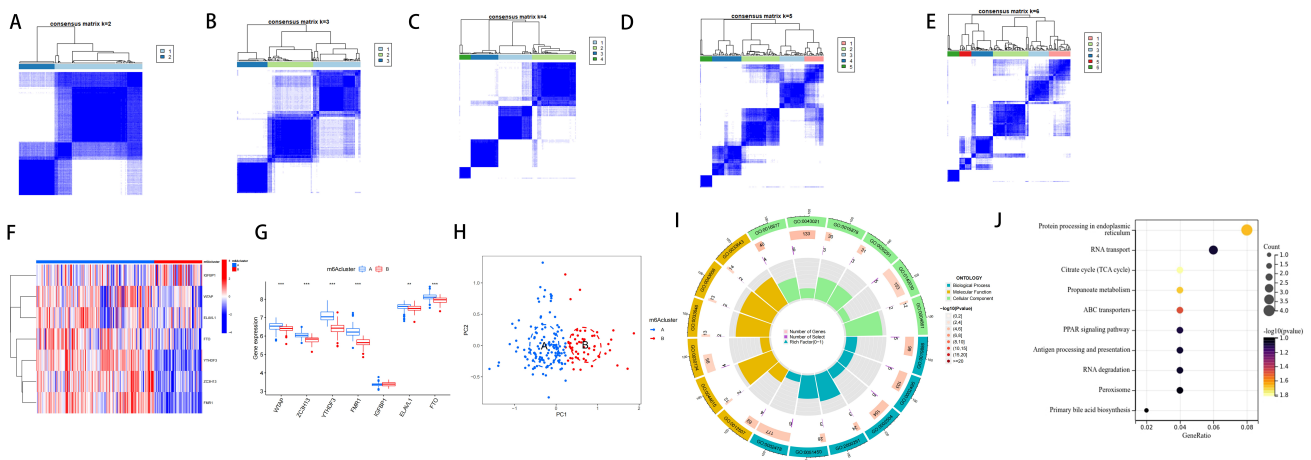


Fig. 5. Consensus clustering of the seven selected m6A regulators in chronic HF patients. (A–E) Consensus matrices of the 7 significant m6A regulators for $k = 2-6$. (F) Expression heat map of the 7 selected m6A regulators in clusters A and B. (G) Differential expression histogram of the 7 selected m6A regulators in clusters A and B. (H) Principal component analysis for the expression profiles of the 7 selected m6A regulators shows a marked difference in the transcriptomes between the two m6A clusters. (I) GO FEA was performed to investigate the possible mechanisms involving the 117 DEGs in CHF. (J) KEGG analysis revealed potential signaling pathways for the DEGs involved in CHF. ** $p < 0.01$, and *** $p < 0.001$. GO, Gene Ontology; DEGs, differentially expressed genes; KEGG, Kyoto Encyclopedia of Genes and Genomes.

between the two clusters (Fig. 5F,G). The ELs of *WTAP*, *ZC3H13*, *YTHDF3*, *FMR1*, *ELAVL1*, and *FTO* were higher in cluster A than cluster B, whereas the EL of *IGFBP1* did

not differ between the two groups. PCA confirmed that the 7 selected m6A regulators clearly formed two distinct cluster patterns (Fig. 5H). GO FEA revealed the 117 DEGs

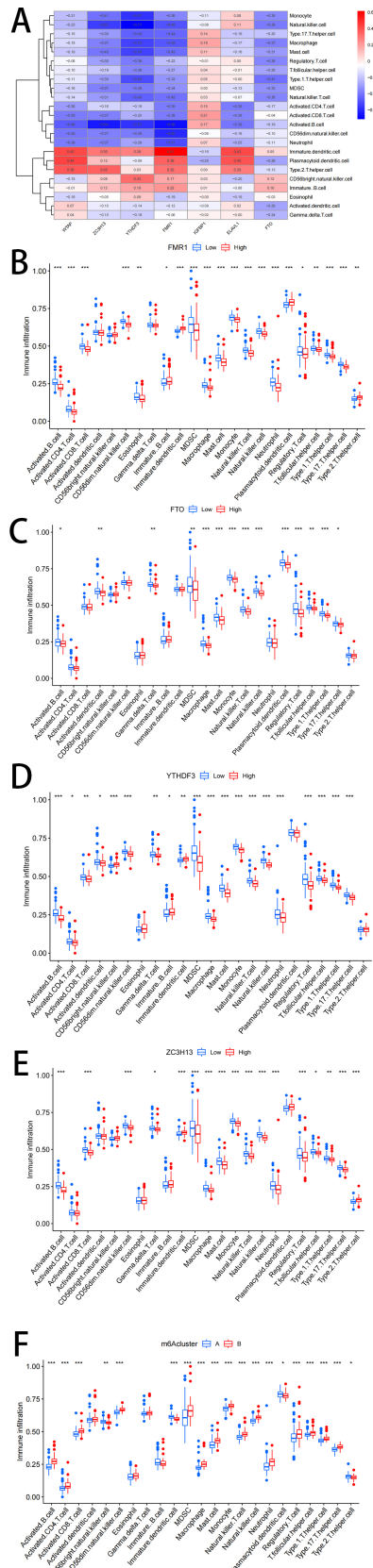


Fig. 6. Single sample gene set enrichment analysis. (A) Correlations between infiltrating immune cells and the 7 selected m6A regulators. (B–E) Differences in the abundance of infiltrating immune cells between the high and low expression groups for *FMR1*, *FTO*, *YTHDF3*, *ZC3H13*. (F) Differential immune cell infiltration between cluster A and cluster B. * $p < 0.05$, ** $p < 0.01$, and *** $p < 0.001$.

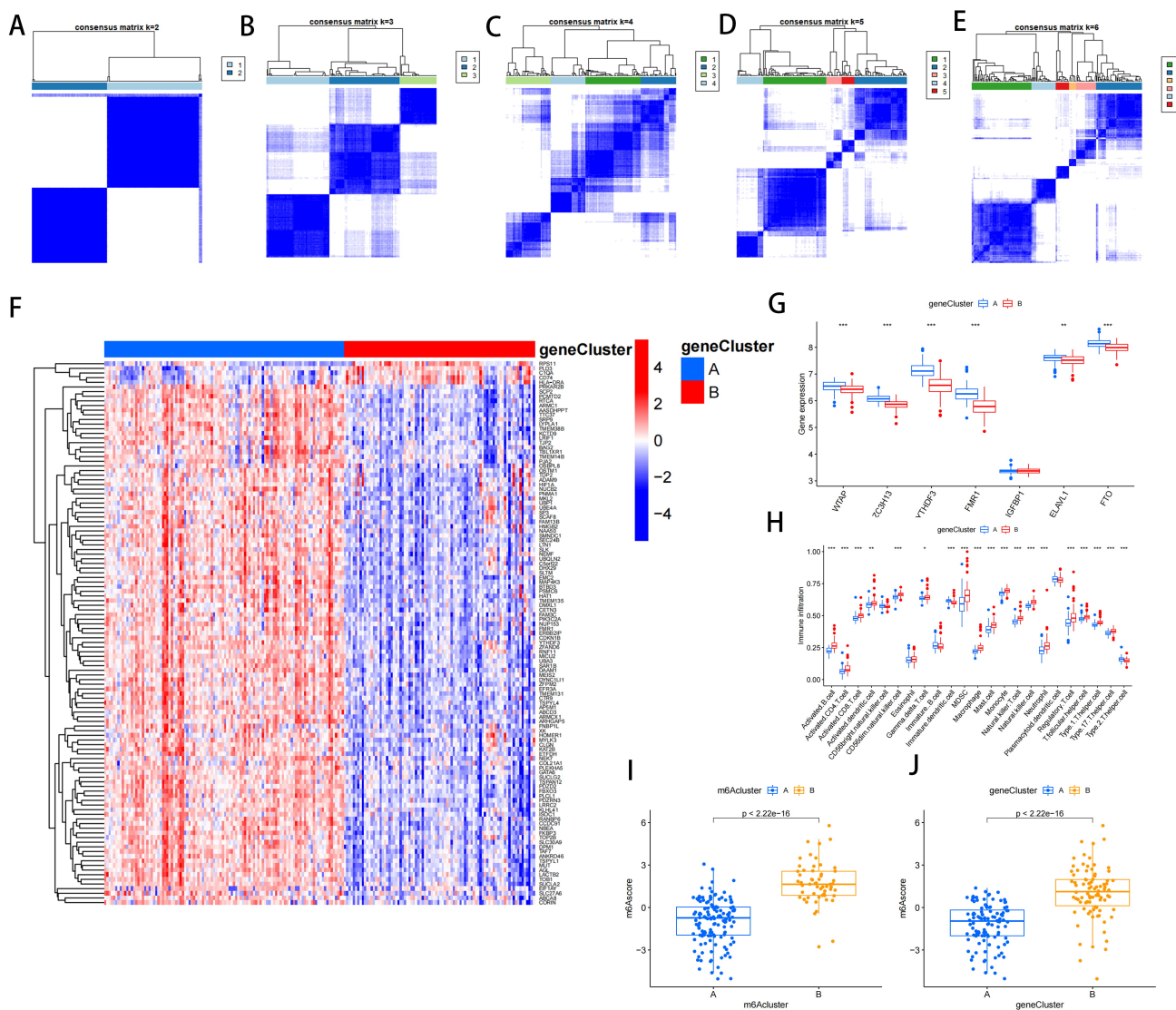


Fig. 7. Consensus clustering of the 117 DEGs in CHF patients. (A–E) Consensus matrices of the 117 DEGs for $k = 2$ –6. (F) Expression heat map of the 117 DEGs in gene cluster A (GCA) and gene cluster B (GCB). (G) Differential expression of the 7 selected m6A regulators between GCA and GCB. (H) Differential immune cell infiltration between GCA and GCB. (I) Differences in the m6A score between cluster A and cluster B. (J) Differences in the m6A score between GCA and GCB. * $p < 0.05$, ** $p < 0.01$, and *** $p < 0.001$. DEGs, differentially expressed genes.

(in cluster A and cluster B combined) that were associated with the 7 m6A regulators were mainly enriched for the GO terms “antigen processing and presentation of exogenous peptide antigen” (GO:0002478) and “ribonucleoprotein complex binding” (GO:0043021) (Fig. 5I). KEGG analysis revealed the DEGs were mainly enriched for protein processing in the endoplasmic reticulum, RNA transport, and the citrate cycle (TCA cycle) (Fig. 5J).

Relationship between m6A Regulators and Immune Cells

ssGSEA was utilized to determine immune cell abundance in the CHF samples and also to investigate associations between the selected m6A regulators and immune cells. The ELs of the m6A regulators were upregulated

in the CHF group, while the ELs of *ZC3H13*, *YTHDF3*, *FMRI*, and *FTO* were negatively associated with many of the immune cell types (Fig. 6A). Differences in immune cell infiltration between patients with high or low ELs of *ZC3H13*, *YTHDF3*, *FMRI*, and *FTO* were also investigated. Patients with low ELs of *ZC3H13*, *YTHDF3*, *FMRI*, and *FTO* showed increased infiltration of immune cells (Fig. 6B–E). In addition, cluster A was associated with Th2-dominant immunity, whereas cluster B was related to Th1-, monocyte-, and macrophage-dominant immunity (Fig. 6F).

Identification of Two Distinct Gene Clusters Based on the Association of DEGs with Seven Selected m6A Regulators

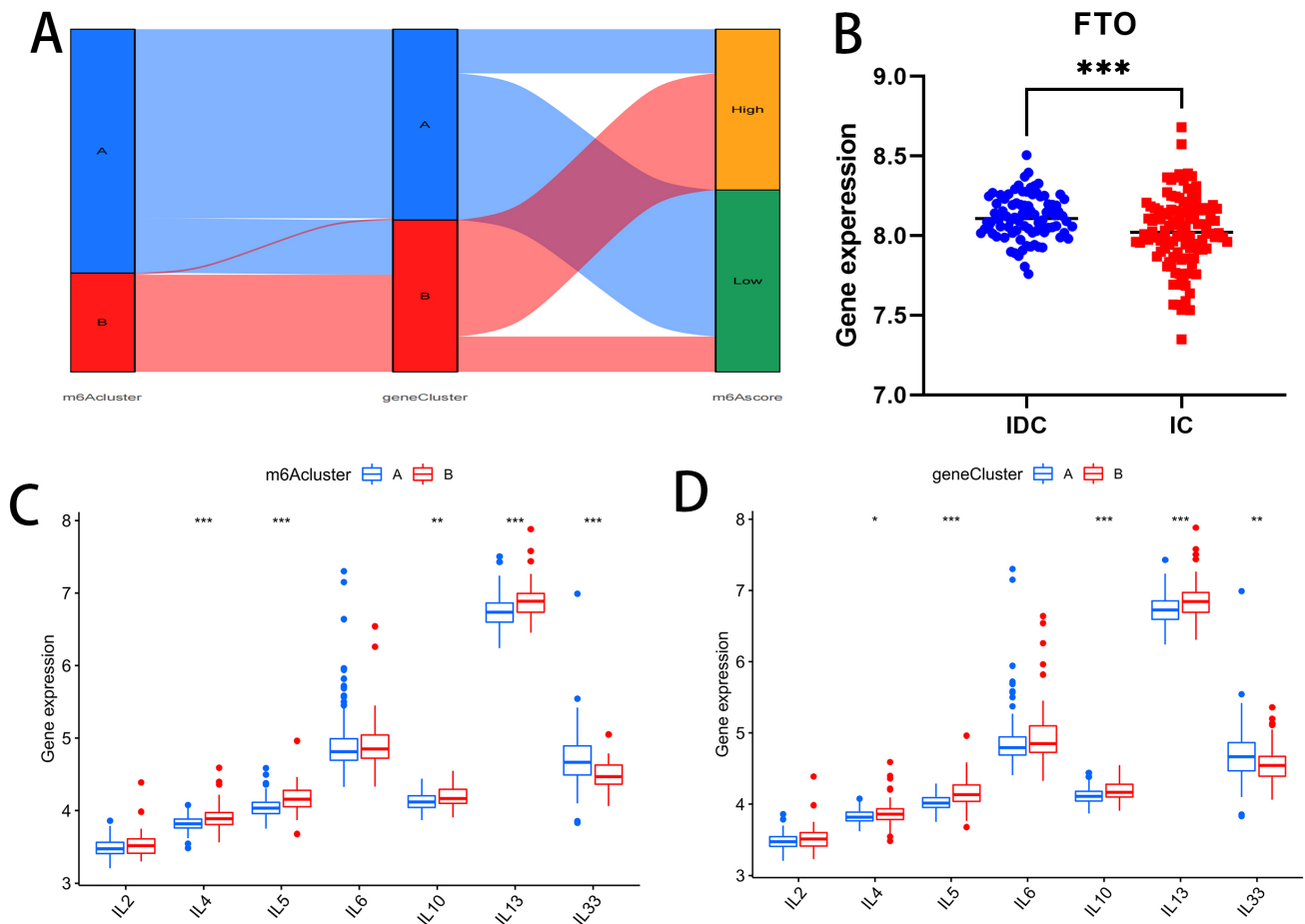


Fig. 8. Predictive ability of different m6A groups for distinguishing CHF. (A) Sankey diagram showing the relationship between m6A cluster A and cluster B, m6A GCA and GCB, and m6A scores. (B) ELs of *FTO* in different types of HF. (C) Differential ELs of *IL-2*, *IL-4*, *IL-5*, *IL-6*, *IL-10*, *IL-13* and *IL-33* between m6A cluster A and cluster B. (D) Differential ELs of *IL-2*, *IL-4*, *IL-5*, *IL-6*, *IL-10*, *IL-13* and *IL-33* between GCA and GCB. * $p < 0.05$, ** $p < 0.01$, and *** $p < 0.001$, IDC, idiopathic dilated cardiomyopathy; IC, ischemic cardiomyopathy.

To further validate the m6A expression clusters A and B, a consensus clustering method was used to classify the CHF patients into different subgroups according to the DEGs. This revealed two distinct m6A gene expression patterns, GCA and GCB, with 108 and 86 samples, respectively (Fig. 7A–E). ELs for the 117 m6A regulator-associated DEGs in GCA and GCB are shown as a heat map in Fig. 7F. Differential ELs of the 7 selected m6A regulators in the GCA and GCB groups, as well as the differential immune cell infiltration in GCA and GCB, were similar to those detected in the m6A regulator cluster A and cluster B groups described above (Fig. 7G,H), thereby confirming the accuracy of the consensus clustering-based groupings.

PCA was utilized to calculate the m6A scores of each sample and to quantify and compare the different m6A patterns (cluster A, cluster B, GCA, GCB). The m6A scores in cluster B and GCB were higher than those of cluster A and GCA (Fig. 7I,J). The relationships between m6A cluster A and B, GCA and GCB, and m6A scores are illustrated using a Sankey diagram (Fig. 8A). The EL of *FTO* in the

idiopathic dilated cardiomyopathy HF group was markedly higher than in the ischemic HF group. However, no major differences in the ELs of the other 6 m6A regulators were apparent between the two HF groups (Fig. 8B). We also investigated possible relationships between the m6A pattern (cluster A, cluster B, GCA, GCB) and the ELs for *IL-2*, *IL-4*, *IL-5*, *IL-6*, *IL-10*, *IL-13*, and *IL-33* (Fig. 8C,D). The ELs for *IL-4*, *IL-5*, *IL-10*, and *IL-13* were higher in m6A cluster B and GCB than in m6A cluster A and GCA. In contrast, the EL for *IL-33* was higher in m6A cluster A and GCA than in m6A cluster B and GCB. The EL for *IL-2* did not differ between the different m6A clusters. The increased Th1/Th2 cytokine ratio observed in m6A cluster B and GCB may be associated with ischemic HF. Patients in the m6A cluster B and GCB groups may experience more release of proinflammatory cytokines, and hence the degree of inflammation would be more severe than in m6A cluster A and GCA patients.

Discussion

CHF is a complex cardiac syndrome caused by structural and functional disorders that affect the ability of the heart to deliver oxygen to tissues. The incidence of CHF is expected to keep rising over the coming years due to the aging populations in many countries [16]. CHF markedly reduces patient quality of life and places enormous pressure on healthcare systems around the world [17]. m6A appears to play a major role in heart disease [7,18]. However, to date the regulatory mechanisms associated with m6A genes in CHF have not been studied in detail.

In the current study, 20 m6A regulators were identified in CHF and HC groups within the GEO. Amongst these, 7 differentially expressed m6A regulators (writers: *WTAP*, *ZC3H13*; readers: *YTHDF3*, *FMRI*, *IGFBP1*, and *ELAVL1*; eraser: *FTO*) were selected for further analysis. The ELs of *RBM15* and *ZC3H13* were positively correlated with the EL of *FTO*. Moreover, the ELs of *FTO* and *ZC3H13* were higher in the CHF group than in the HC group. No difference in the EL of *RBM15* was found between the two groups. The ability of the 7 selected m6A regulators to predict CHF risk was evaluated using RF and nomogram models. DCA indicated that patients could derive benefit from predictions made using the nomogram model. *WTAP* codes for a regulatory subunit of the METTL3–METTL14 complex that binds to mRNA [19]. It is known to promote myocardial infarction via the regulation of activating transcription factor 4 [20]. The *ZC3H13* gene product promotes malignant behavior in hepatoma carcinoma cells through PKM2-dependent glycolysis signaling [10]. The role of *ZC3H13* in the heart remains unclear, however. The *YTHDF3* gene product functions in synergy with *YTHDF1* to facilitate protein synthesis and influence *YTHDF2*-mediated decay of methylated mRNA [21]. Overexpression of *FMRI* reduces oxidative stress and apoptosis of LPS-injured H9c2 cardiomyocytes through the PI3K/Akt pathway [11]. CHF can be identified based on the plasma *IGFBP-1* concentration and *IGFBP-1/IGF-1* ratio [22]. *IGFBP1* therefore has potential value in the diagnosis of CHF. The *ELAVL1* gene product inhibits hyperglycemia-induced apoptosis of human ventricular cardiomyocytes [23]. The overexpression of *FTO* reduces fibrosis and enhances angiogenesis. Furthermore, *FTO* is involved in cardiac systolic function during vascular remodeling and regeneration [8]. In summary, the m6A regulator genes identified in the present study play key roles in cardiac function. The current results are in line with those of previous studies, and identify several possible diagnostic and therapeutic targets for further research on CHF.

Inflammatory mediators are active during the pathogenesis of CHF, leading to cardiac remodeling and peripheral vascular dysfunction [24]. Studies have shown that *IL-4*, *IL-5*, *IL-10*, and *IL-13* are involved in the regula-

tion of cardiac function [25]. For example, serum *IL-4* levels in patients with acute myocardial infarction after percutaneous coronary therapy have good diagnostic value for the impairment of left ventricular function [26]. *IL-5* has a cardioprotective role in infarcted myocardium by promoting eosinophil accumulation and subsequent polarization of *CD206*⁺ macrophages via the *IL-4/STAT6* axis [27]. *IL-10* is secreted by macrophages to increase the number of myeloid-derived suppressor cells, thereby protecting the heart [28]. *IL-13* participates in host protection by promoting tissue repair and controlling inflammatory processes [29], while also being a key determinant of the fate of cardiac myocytes. Moreover, *IL-13* is reverse transcribed during cardiogenesis and has cardioprotective effects [30]. *IL-33* levels have predictive value in patients with CHF and acute myocardial infarction [31]. Some studies have suggested that a Th1 response may occur in human end-stage HF [32]. In addition, emotional and autonomic nervous system imbalances have been associated with increased systemic inflammation in elderly patients suffering from decompensated CHF [33]. In the present study, the ELs of *IL-4*, *IL-5*, *IL-10*, and *IL-13* were elevated in m6A cluster B and GCB, whereas the EL of *IL-33* was elevated in m6A cluster A and GCA. Based on the above literature and findings, we speculate that the high ELs of many inflammatory cytokines in m6A cluster B and GCB may indicate the presence of a severe inflammatory response or advanced HF in these patient groups.

The Th1 immune response is proinflammatory, kills intracellular microorganisms, and contributes to the autoimmune response, whereas the Th2 immune response is anti-inflammatory, inhibits the cellular immune response, and promotes the humoral immune response [34]. Monocytes protect the body from harmful pathogens by removing them via phagocytosis. Moreover, they are considered to be the main source of various cytokines, macrophages, and dendritic cell precursors [35]. Inflammation and the maintenance of chronic inflammation rely heavily on the presence of monocytes and activated macrophages, as well as the cytokines they produce [36]. Monocytes are generally divided into three subtypes, namely Mon1, Mon2, and Mon3. Mon1 cells can induce the inflammatory response and phagocytosis. Mon2 cells participate in the inflammatory process through antigen presentation, cytokine secretion, apoptosis regulation, and by their influence on angiogenic activity. Mon3 cells function in *Fcγ* receptor-mediated phagocytosis and neutrophil adhesion at the endothelial interface. Mon2 cells may be involved in maintaining chronic inflammation, leading to the harmful remodeling of heart tissue [37]. Mon1 cells have higher phagocytotic activity than Mon3 cells, and play active roles in the initiation, development, and regression of tissue inflammation [38]. Elevated ELs of Mon2 markers and decreased ELs of Mon1 markers in CHF patients are associated with the severity of HF [39].

In the present study, ELs for Th1 immunity were found to be upregulated in m6A cluster B and GCB compared to m6A cluster A and GCA. In contrast, the ELs for Th2 immunity were downregulated in m6A cluster B and GCB compared to m6A cluster A and GCA. The increased Th1/Th2 ratio suggests that patients in the m6A cluster B and GCB groups may experience an elevated release of proinflammatory cytokines. Hence, the degree of inflammation in these patients would be more severe than that experienced by patients in the m6A cluster A and GCA groups. The levels of inflammatory markers are known to be markedly elevated in patients with advanced HF compared to the normal population, suggesting that chronic, low-level inflammation is a hallmark of CHF [40]. In the current study, the high levels of inflammation observed in m6A cluster B and GCB may be indicative of ischemic HF, since this disease leads to severe heart damage. Based on our findings, we suggest that anti-inflammatory processes which can reduce vascular inflammation and regulate the monocyte/macrophage system may represent therapeutic targets in CHF.

Conclusion

We identified 7 candidate m6A regulators and developed a nomogram model to predict CHF. Two clear m6A patterns were revealed using these 7 markers, one of which (cluster B/GCB) may be indicative of ischemic HF.

Limitations

The raw data analyzed in this study were uploaded several years ago. Therefore, more recently identified m6A genes such as *ALKBH5* and *METTL14* were not included in the analysis. In addition, a suitable dataset for the verification of our results was not found. Finally, the number of disease samples in the cluster B and GCB groups was different.

Abbreviations

m6A, RNA N6-methyladenosine; CHF, chronic heart failure; GEO database, Gene Expression Omnibus database; WTAP, Wilms' tumor 1-associating protein; ZC3H13, zinc finger CCCH-type containing 13; YTHDF3, YTH N6-methyladenosine RNA binding protein 1; FMR1, fragile X mental retardation 1; IGFBP1, insulin-like growth factor-binding protein 1; ELAVL1, ELAV-like protein 1; FTO, fat mass and obesity-associated protein; HC group, the healthy control group; RF model, random forest model; SVM model, support vector machine model; ROC curve, receiver operating characteristic curve; DCA, decision

curve analysis; PCA, principal component analysis; DEG, differentially expressed gene; ssGSEA, single-sample gene set enrichment analysis; GO, Gene Ontology; KEGG, Kyoto Encyclopedia of Genes and Genomes.

Consent for Publication

Not applicable.

Availability of Data and Materials

GEO data (ID:200005406) can be obtained from the website (<https://www.ncbi.nlm.nih.gov/geo/query/acc.cgi?acc=GSE5406>). The datasets used and/or analyzed during the current study are available from the corresponding author on reasonable request.

Author Contributions

FZ, YY, WY and RB contributed to the conception and design of the research and drafted the manuscript. YL, JC, and SW contributed to data collection. NL and XL analyzed the data and prepared figures. WY and RB revised the manuscript. All authors contributed to critical revision of the manuscript and approved its final version. All authors have participated sufficiently in the work to take public responsibility for appropriate portions of the content and agreed to be accountable for all aspects of the work in ensuring that questions related to its accuracy or integrity.

Ethics Approval and Consent to Participate

Not applicable.

Acknowledgment

Not applicable.

Funding

This research received no external funding.

Conflict of Interest

The authors declare no conflict of interest.

References

- [1] McDonagh TA, Metra M, Adamo M, Gardner RS, Baumbach A, Böhm M, *et al.* 2021 ESC Guidelines for the diagnosis and treatment of acute and chronic heart failure. *European Heart Journal.* 2021; 42: 3599–3726.
- [2] Qin Y, Li L, Luo E, Hou J, Yan G, Wang D, *et al.* Role of m6A RNA methylation in cardiovascular disease (Review). *International Journal of Molecular Medicine.* 2020; 46: 1958–1972.
- [3] Roignant JY, Soller M. m⁶A in mRNA: An Ancient Mechanism for Fine-Tuning Gene Expression. *Trends in Genetics: TIG.* 2017; 33: 380–390.
- [4] Hershberger RE, Givertz MM, Ho CY, Judge DP, Kantor PF, McBride KL, *et al.* Genetic Evaluation of Cardiomyopathy-A Heart Failure Society of America Practice Guideline. *Journal of Cardiac Failure.* 2018; 24: 281–302.
- [5] Hershberger RE, Givertz MM, Ho CY, Judge DP, Kantor PF, McBride KL, *et al.* Genetic evaluation of cardiomyopathy: a clinical practice resource of the American College of Medical Genetics and Genomics (ACMG). *Genetics in Medicine: Official Journal of the American College of Medical Genetics.* 2018; 20: 899–909.
- [6] Kayvanpour E, Sammani A, Sedaghat-Hamedani F, Lehmann DH, Broezel A, Koelemenoglu J, *et al.* A novel risk model for predicting potentially life-threatening arrhythmias in non-ischemic dilated cardiomyopathy (DCM-SVA risk). *International Journal of Cardiology.* 2021; 339: 75–82.
- [7] Berulava T, Buchholz E, Elerdashvili V, Pena T, Islam MR, Lbik D, *et al.* Changes in m6A RNA methylation contribute to heart failure progression by modulating translation. *European Journal of Heart Failure.* 2020; 22: 54–66.
- [8] Mathiyalagan P, Adamiak M, Mayourian J, Sassi Y, Liang Y, Agarwal N, *et al.* FTO-Dependent N⁶-Methyladenosine Regulates Cardiac Function During Remodeling and Repair. *Circulation.* 2019; 139: 518–532.
- [9] Zhang B, Wu Q, Li B, Wang D, Wang L, Zhou YL. m⁶A regulator-mediated methylation modification patterns and tumor microenvironment infiltration characterization in gastric cancer. *Molecular Cancer.* 2020; 19: 53.
- [10] Wang Q, Xie H, Peng H, Yan J, Han L, Ye G. ZC3H13 Inhibits the Progression of Hepatocellular Carcinoma through m⁶A-PKM2-Mediated Glycolysis and Enhances Chemosensitivity. *Journal of Oncology.* 2021; 2021: 1328444.
- [11] Bao J, Ye C, Zheng Z, Zhou Z. Fmr1 protects cardiomyocytes against lipopolysaccharide-induced myocardial injury. *Experimental and Therapeutic Medicine.* 2018; 16: 1825–1833.
- [12] Zhu B, Gong Y, Shen L, Li J, Han J, Song B, *et al.* Total Panax notoginseng saponin inhibits vascular smooth muscle cell proliferation and migration and intimal hyperplasia by regulating WTAP/p16 signals via m⁶A modulation. *Biomedicine & Pharmacotherapy.* 2020; 124: 109935.
- [13] Anversa P, Reiss K, Kajstura J, Cheng W, Li P, Sonnenblick EH, *et al.* Myocardial infarction and the myocyte IGF1 autocrine system. *European Heart Journal.* 1995; 16: 37–45.
- [14] Wang S, Zhang J, Wu X, Lin X, Liu XM, Zhou J. Differential roles of YTHDF1 and YTHDF3 in embryonic stem cell-derived cardiomyocyte differentiation. *RNA Biology.* 2021; 18: 1354–1363.
- [15] Cao S, Li C, Li L, Zhou G, Jiang Y, Feng J. Circular RNA hsa_circ_0000848 Regulates Cardiomyocyte Proliferation and Apoptosis Under Hypoxia via Recruiting ELAVL1 and Stabilizing SMAD7 mRNA. *Anatolian Journal of Cardiology.* 2022; 26: 189–197.
- [16] Rogers C, Bush N. Heart Failure: Pathophysiology, Diagnosis, Medical Treatment Guidelines, and Nursing Management. *The Nursing Clinics of North America.* 2015; 50: 787–799.
- [17] Alem MM. Endothelial Dysfunction in Chronic Heart Failure: Assessment, Findings, Significance, and Potential Therapeutic Targets. *International Journal of Molecular Sciences.* 2019; 20: 3198.
- [18] Xue T, Qiu X, Liu H, Gan C, Tan Z, Xie Y, *et al.* Epigenetic regulation in fibrosis progress. *Pharmacological Research.* 2021; 173: 105910.
- [19] Zhang B, Jiang H, Dong Z, Sun A, Ge J. The critical roles of m6A modification in metabolic abnormality and cardiovascular diseases. *Genes & Diseases.* 2020; 8: 746–758.
- [20] Wang J, Zhang J, Ma Y, Zeng Y, Lu C, Yang F, *et al.* WTAP promotes myocardial ischemia/reperfusion injury by increasing endoplasmic reticulum stress via regulating m⁶A modification of ATF4 mRNA. *Aging.* 2021; 13: 11135–11149.
- [21] Shi H, Wang X, Lu Z, Zhao BS, Ma H, Hsu PJ, *et al.* YTHDF3 facilitates translation and decay of N⁶-methyladenosine-modified RNA. *Cell Research.* 2017; 27: 315–328.
- [22] Guo S, Gong M, Tse G, Li G, Chen KY, Liu T. The Value of IGF-1 and IGFBP-1 in Patients With Heart Failure With Reduced, Mid-range, and Preserved Ejection Fraction. *Frontiers in Cardiovascular Medicine.* 2022; 8: 772105.
- [23] Jeyabal P, Thandavarayan RA, Joladarashi D, Suresh Babu S, Krishnamurthy S, Bhimaraj A, *et al.* MicroRNA-9 inhibits hyperglycemia-induced pyroptosis in human ventricular cardiomyocytes by targeting ELAVL1. *Biochemical and Biophysical Research Communications.* 2016; 471: 423–429.
- [24] Gullestad L, Ueland T, Vinge LE, Finsen A, Yndestad A, Aukrust P. Inflammatory cytokines in heart failure: mediators and markers. *Cardiology.* 2012; 122: 23–35.
- [25] Bartekova M, Radosinska J, Jelemensky M, Dhalla NS. Role of cytokines and inflammation in heart function during health and disease. *Heart Failure Reviews.* 2018; 23: 733–758.
- [26] Szkodzinski J, Hudzik B, Osuch M, Romanowski W, Szygula-Jurkiewicz B, Polonski L, *et al.* Serum concentrations of interleukin-4 and interferon-gamma in relation to severe left ventricular dysfunction in patients with acute myocardial infarction undergoing percutaneous coronary intervention. *Heart and Vessels.* 2011; 26: 399–407.
- [27] Xu JY, Xiong YY, Tang RJ, Jiang WY, Ning Y, Gong ZT, *et al.* Interleukin-5-induced eosinophil population improves cardiac function after myocardial infarction. *Cardiovascular Research.* 2022; 118: 2165–2178.
- [28] Feng L, Li G, An J, Liu C, Zhu X, Xu Y, *et al.* Exercise Training Protects Against Heart Failure Via Expansion of Myeloid-Derived Suppressor Cells Through Regulating IL-10/STAT3/S100A9 Pathway. *Circulation: Heart Failure.* 2022; 15: e008550.
- [29] Gause WC, Wynn TA, Allen JE. Type 2 immunity and wound healing: evolutionary refinement of adaptive immunity by helminths. *Nature Reviews: Immunology.* 2013; 13: 607–614.
- [30] O'Meara CC, Wamstad JA, Gladstone RA, Fomovsky GM, Butty VL, Shrikumar A, *et al.* Transcriptional reversion of cardiac myocyte fate during mammalian cardiac regeneration. *Circulation Research.* 2015; 116: 804–815.
- [31] Xing J, Liu J, Geng T. Predictive values of sST2 and IL-33 for heart failure in patients with acute myocardial infarction. *Experimental Biology and Medicine (Maywood, N.J.).* 2021; 246: 2480–2486.
- [32] Athanassopoulos P, Vaessen LMB, Maat APWM, Balk AHMM, Weimar W, Bogers AJJC. Peripheral blood dendritic cells in human end-stage heart failure and the early post-transplant period: evidence for systemic Th1 immune responses. *European Journal of Cardio-thoracic Surgery: Official Journal of the European Association for Cardio-thoracic Surgery.* 2004; 25: 619–626.
- [33] Guinjoan SM, Vigo DE, Castro MN, Tateosian N, Chuluyan E, Costanzo E, *et al.* Mood, Th-1/Th-2 cytokine profile, and auto-

- nostic activity in older adults with acute/decompensated heart failure: preliminary observations. *The World Journal of Biological Psychiatry: the Official Journal of the World Federation of Societies of Biological Psychiatry*. 2009; 10: 913–918.
- [34] Gage JR, Fonarow G, Hamilton M, Widawski M, Martínez-Maza O, Vredevoe DL. Beta blocker and angiotensin-converting enzyme inhibitor therapy is associated with decreased Th1/Th2 cytokine ratios and inflammatory cytokine production in patients with chronic heart failure. *Neuroimmunomodulation*. 2004; 11: 173–180.
- [35] Mongirdienė A, Liobikas J. Phenotypic and Functional Heterogeneity of Monocyte Subsets in Chronic Heart Failure Patients. *Biology*. 2022; 11: 195.
- [36] Ridker PM, Lüscher TF. Anti-inflammatory therapies for cardiovascular disease. *European Heart Journal*. 2014; 35: 1782–1791.
- [37] Boyette LB, Macedo C, Hadi K, Elinoff BD, Walters JT, Ramaswami B, *et al.* Phenotype, function, and differentiation potential of human monocyte subsets. *PLoS ONE*. 2017; 12: e0176460.
- [38] Serbina NV, Cherny M, Shi C, Bleau SA, Collins NH, Young JW, *et al.* Distinct responses of human monocyte subsets to *Aspergillus fumigatus* conidia. *Journal of Immunology (Baltimore, Md.: 1950)*. 2009; 183: 2678–2687.
- [39] Barisione C, Garibaldi S, Ghigliotti G, Fabbi P, Altieri P, Casale MC, *et al.* CD14CD16 monocyte subset levels in heart failure patients. *Disease Markers*. 2010; 28: 115–124.
- [40] Everett BM, Cornel JH, Lainscak M, Anker SD, Abbate A, Thuren T, *et al.* Anti-Inflammatory Therapy With Canakinumab for the Prevention of Hospitalization for Heart Failure. *Circulation*. 2019; 139: 1289–1299.